Phosphorus-enhanced diffusion of antimony due to generation of self-interstitials

P. Pichler[a)]
Fraunhofer-Institut für Integrierte Schaltungen, Bereich Bauelementetechnologie, Schottkystrasse 10, D-91058 Erlangen, Germany

H. Ryssel
Fraunhofer-Institut für Integrierte Schaltungen, Bereich Bauelementetechnologie, Schottkystrasse 10, D-91058 Erlangen, Germany, and Lehrstuhl für Elektronische Bauelemente, Universität Erlangen-Nürnberg, Cauerstrasse 6, D-91058 Erlangen, Germany

R. Ploss
Siemens Bauelemente OHG, Siemensstrasse 2, A-9500 Villach, Austria

C. Bonafos and A. Claverie
CEMES/LOE-CNRS, 29 rue Jeanne Mavig, F-31055 Toulouse Cedex, France

(Received 23 February 1995; accepted for publication 7 April 1995)

In a series of experiments, the influence of phosphorus diffusion at high concentrations on the diffusion of an antimony marker layer was investigated. The marker layer was separated from the surface by a 4 μm layer of epitaxially grown silicon. To reduce the effects of implantation enhancement and phosphorus precipitation on the diffusion of the antimony marker layer, the phosphorus was implanted into a polysilicon layer deposited on top of the single-crystalline substrate. It was found that the diffusion of the antimony marker layer is already reduced by the epilayer. From these diffusion coefficients, upper limits for the fractional diffusivity of antimony were derived. In contrast to previous investigations, the diffusion of the antimony marker layer was found to be enhanced below regions where phosphorus was implanted. A comparison of diffusion in FZ and CZ samples shows that this enhanced diffusion of antimony can be explained only by an injection of self-interstitials from the phosphorus-doped region. Since the polysilicon layer was found to recrystallize, this self-interstitial injection can be the result of phosphorus diffusing mainly via self-interstitials, phosphorus precipitation, or both. Using Boltzmann–Matano analysis and antimony diffusivity data, the fractional diffusivity of phosphorus via self-interstitials was estimated to be lower than 0.71 at 950 °C. Possible sources of error in this estimation are discussed.

I. INTRODUCTION

The so-called emitter dip effect or emitter push effect[1] was already observed in the early 1960s. Phosphorus being present in high concentrations at the surface causes enhanced diffusion of gallium and boron in regions separated spatially. Also, since the publication of Tannenbaum,[2] various anomalous effects were reported for the diffusion of phosphorus at high concentrations with the formation of a clearly visible kink in the diffusion profiles as the most prominent anomaly.[3] In the models of Yoshida[4] and Fair and Tsai,[5] it was assumed that phosphorus–vacancy pairs, the so-called E centers, are formed in regions with high phosphorus concentrations. These pairs are assumed to be mobile and to dissolve in regions with low phosphorus concentrations. This dissolution liberates vacancies which act as diffusion vehicles for the dopants and thus enhances the effective diffusion coefficient of the phosphorus ions.

Such models based on the long-ranging interaction of dopants and one species of diffusion vehicles could explain the enhanced diffusion of boron and phosphorus observed, e.g., during oxidation or below regions with high phosphorus concentrations. However, they could not explain the retarded diffusion of antimony observed at the same time in some experiments. This discrepancy was avoided by the assumption of Seeger and Chik[6] who introduced the idea that self-diffusion and dopant diffusion is moderated by the interaction of dopants with vacancies as well as self-interstitials.

The core of the discussions since then was devoted to the extent of diffusion via these two intrinsic point defects. This question can be solved sufficiently well for antimony since from TEM analysis it is known that agglomerates of self-interstitials are generated during thermal oxidation of silicon.[7] Besides agglomerating to extended defects, self-interstitials generated during thermal oxidation will recombine with vacancies, causing their concentration to drop below the equilibrium value. Since antimony present in intrinsic concentrations was found to diffuse slower under these conditions than in inert ambient, it is a straightforward conclusion that antimony diffusion under intrinsic conditions takes place preferentially via vacancies as diffusion vehicles.

For boron and phosphorus, no general consensus could be achieved so far. One milestone was the work of Fahey *et al.*[8] on silicon nitridation which indicates that phosphorus at 1100 °C and intrinsic concentrations diffuses nearly entirely via self-interstitials. However, the mechanism involved in point defect generation during silicon nitridation is still under discussion. On the other hand, from their work on high-concentration diffusion of phosphorus and boron,

[a)]Electronic mail: pichler@iis-b.fhg.de

Mathiot and Pfister[9] concluded that both dopants diffuse preferentially, but not entirely, via vacancies. We feel that both results for the fractional diffusivity via self-interstitials are not necessarily in contradiction since the work of Fahey *et al.* was concerned with intrinsic concentrations whereas the parameters of Mathiot and Pfister come mainly from diffusion experiments carried out under strongly extrinsic conditions.

Additional evidence was established by experiments where the diffusion of antimony was found to be retarded by phosphorus diffusion at high concentrations.[10] This indicates unambiguously the generation of self-interstitials and was explained generally by phosphorus diffusing at high concentrations primarily via pairs with self-interstitials. However, it could equally well be explained by Mathiot and Pfister[9] on the basis of self-interstitial generation due to the growth of phosphorus precipitates.

The goal of this work was to develop a method to avoid influences of point defects generated by the formation of phosphorus precipitates or the ion implantation process. The idea was to implant the phosphorus into a polysilicon layer deposited on the samples. Self-interstitials generated there are likely to be captured at grain boundaries, especially the grain boundary to the single-crystalline silicon area. Thus an injection of point defects into the single-crystalline silicon area should be avoided or, at least, largely reduced so that it is possible to separate the point defect generation due to phosphorus diffusion from the other effects mentioned above.

II. EXPERIMENTAL TECHNIQUE

In our experiment, phosphorus-doped (100)-oriented float-zone (FZ) and Czochralski grown (CZ) wafers with resistivities of 4–6 Ω cm were used. The antimony marker layers were produced by ion implantation at an energy of 90 keV to a dose of 4×10^{11} cm^{-2} into CZ wafers and to a dose of 4×10^{13} cm^{-2} into FZ wafers. After the implantation, all wafers were annealed at 950 °C for 30 min to remove the implantation damage. On some of the wafers, approximately 4 μm thick epitaxial layers of silicon were deposited at 1100 °C within 10 min in separate processes for CZ and FZ wafers. On some of these wafers, polysilicon layers of 300 nm were deposited at 620 °C and doped by phosphorus implantation at an energy of 100 keV to doses of 3×10^{16} and 2×10^{17} cm^{-2}. Before the diffusion experiments, all wafers were capped by 330 nm of low-temperature oxide (LTO).

For the diffusion, the wafers were loaded at 800 °C and ramped with 10 K/min to the nominal process temperatures of 950 or 1050 °C. At these temperatures, the wafers were diffused for 28 and 2 h, respectively. Then the furnace was ramped down with 5 K/min to 800 °C where the samples were unloaded. In each of these diffusion steps, one sample without an epitaxial layer, one with an epitaxial layer, and one with an epitaxial layer and a doped polysilicon layer were processed. The samples without an epitaxial layer were used to establish a reference for diffusion of antimony under inert and intrinsic conditions. Diffusion of antimony in the samples with an epitaxial layer was used to characterize the influence of the epitaxial layer and other materials properties.

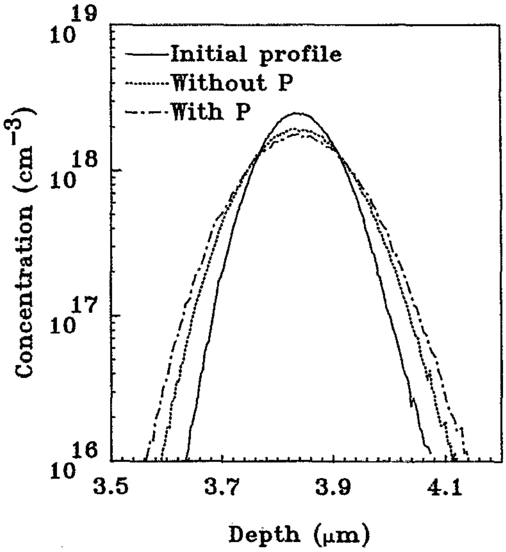

FIG. 1. Initial profile and profiles of antimony after heat treatment at 950 °C for 28 h in FZ samples with an epitaxial layer and with polysilicon doped with a phosphorus dose of 3×10^{16} cm^{-2}.

Finally, the wafers with the additional, doped polysilicon layers were used to study the influence of phosphorus diffusion at high concentrations.

III. MEASURED PROFILES AND PARAMETER EXTRACTION

After removal of the capping LTO layer, the phosphorus and antimony profiles were measured by secondary-ion mass spectroscopy (SIMS) using CAMECA 4*f* equipment. Concentration calibration for the antimony profiles was done via the implanted dose, and via a calibration standard for the phosphorus profiles. The samples were also analyzed by TEM with respect to extended defects which might have an influence on the experiments.

As a typical example, the antimony profiles measured in FZ samples after 28 h at 950 °C are shown in Fig. 1. From these profiles, effective diffusion coefficients were extracted by parameter fitting with ICECREM[11] and listed in Table I. The ramping periods during the diffusion step were included in the simulations assuming an activation energy of 3.98 eV for the intrinsic diffusion coefficient of antimony. For the CZ samples, due to the lower dose implanted, the statistics of SIMS measurements were worse than for the FZ samples. Thus the respective diffusion coefficients have to be taken *cum grano salis* without affecting the general trend. In Fig.

TABLE I. Effective diffusion coefficients of antimony in cm^2/s.

		Without epilayer	Without phosphorus	Phosphorus 3×10^{16} cm^{-2}	Phosphorus 2×10^{17} cm^{-2}
950 °C	FZ	3.8×10^{-16}	1.1×10^{-16}	1.8×10^{-16}	3.9×10^{-16}
	CZ	3.6×10^{-16}	1.2×10^{-16}	2.1×10^{-16}	
1050 °C	FZ	1.0×10^{-14}	4.5×10^{-15}	5.7×10^{-15}	
	CZ	7.9×10^{-15}	2.8×10^{-15}	3.6×10^{-15}	

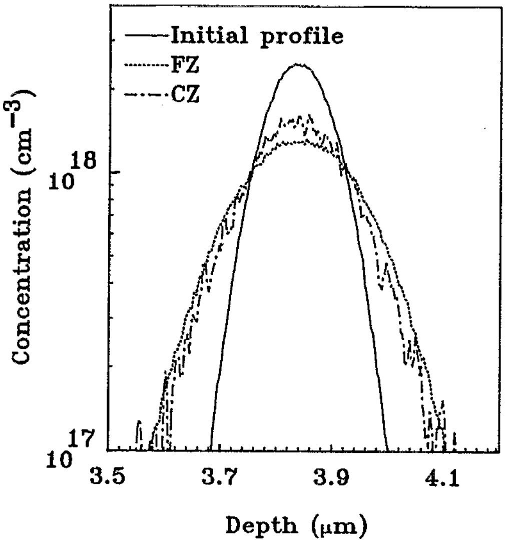

FIG. 2. Initial profile and profiles of antimony after heat treatment at 1050 °C for 2 h in FZ and CZ samples with polysilicon doped with a phosphorus dose of 3×10^{16} cm^{-2}.

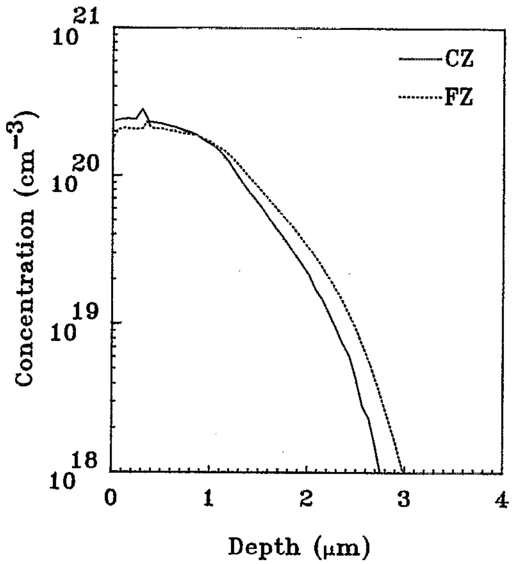

FIG. 4. Profiles of phosphorus after heat treatment at 1050 °C for 2 h.

2, the profiles measured in CZ and FZ samples with implanted phosphorus after 2 h at 1050 °C are shown.

The profiles of phosphorus measured after heat treatment at 950 and 1050 °C in the samples with doped polysilicon are shown in Figs. 3 and 4, respectively. The origin of the depth scale corresponds to the surface of the polysilicon layer. At the position of the interface between polysilicon and silicon, a pileup in the profiles can be seen. The profiles at 950 °C especially show the typical kink and tail which indicate enhanced diffusivity in the tail region and, in consequence, a high supersaturation of either self-interstitials or vacancies.

IV. INVESTIGATIONS BY TRANSMISSION ELECTRON MICROSCOPY

In addition to depth profiling of the dopant profiles, samples with epitaxial layer and samples with the additional polysilicon layer doped with phosphorus to a dose of 3×10^{16} cm^{-2} were analyzed by cross-section transmission electron microscopy (XTEM). The XTEM analysis was performed after the diffusion experiment as well as for samples which were not annealed.

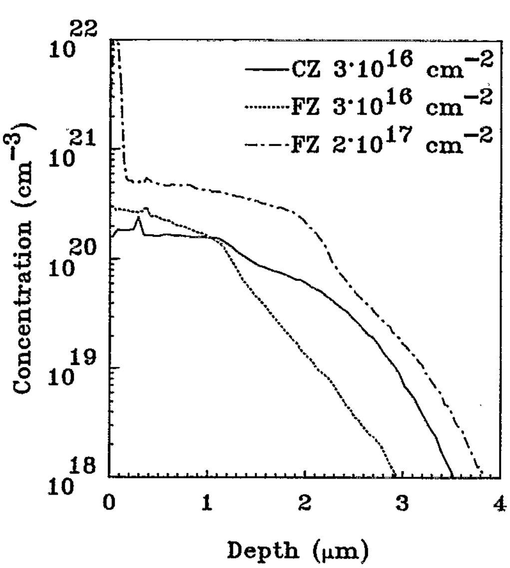

FIG. 3. Profiles of phosphorus after heat treatment at 950 °C for 28 h.

In the unannealed and annealed samples with an epitaxial layer, no extended defects were found. As an example, Fig. 5 shows the sample after annealing at 950 °C for 28 h. Especially at the interface between epitaxially deposited silicon and bulk silicon, defects are not visible. Figures 6 and 7 show the XTEM images of the phosphorus-doped samples after diffusion at 950 °C for 28 h and 1050 °C for 2 h, respectively. In both samples, the epitaxial layer was found to be recrystallized. The very few remaining defects are twins and dislocation loops. This means that the capability of the polysilicon layer to capture point defects was probably largely reduced during these processes.

At the former interface between polysilicon and silicon, the native oxide existing prior to the deposition of the polysilicon has broken up and forms a line of small precipitates. At these precipitates, phosphorus atoms are likely to be pinned, leading to the pileup in the profiles in Figs. 3 and 4.

V. DISCUSSION

Experimental data on the intrinsic diffusion coefficient of antimony are quite rare in the literature. Figure 8 shows the effective diffusion coefficients of antimony in the samples without epitaxial layers together with the data of Fuller and Ditzenberger,[12] Rohan *et al.*,[13] Millea,[14] and Adda.[15] Of the data of Fuller and Ditzenberger only the values for intrinsic concentrations have been included. A regression analysis leads to a diffusion coefficient of antimony in inert ambient under intrinsic conditions of

$$D_0=71.1\ \frac{\mathrm{cm}^2}{\mathrm{s}}\exp\left(-\frac{4.204\ \mathrm{eV}}{kT}\right). \tag{1}$$

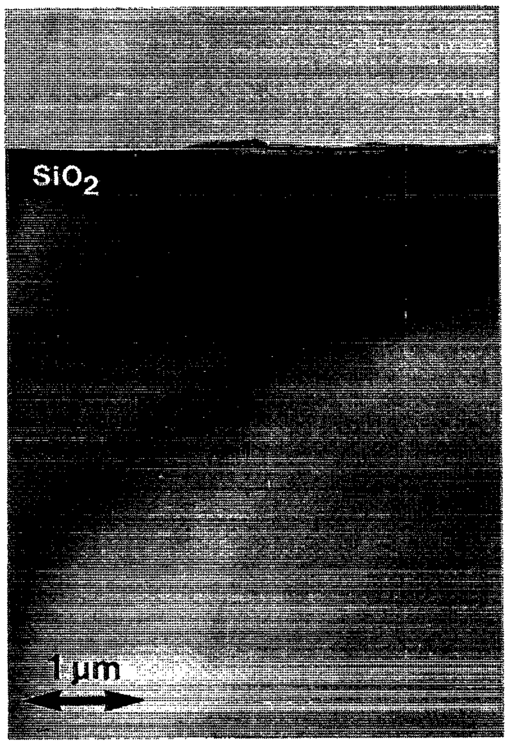

FIG. 5. Bright field XTEM image ($g = 220$) of the sample with an epitaxial layer annealed at 950 °C for 28 h.

At 950 and 1050 °C, the most probable values for the intrinsic diffusion coefficients are 3.38×10^{-16} and 6.89×10^{-15} cm^2/s, respectively. From the data points, 90% confidence and prediction intervals were estimated and included in Fig. 8. The meaning of these intervals is that the true value is with a probability of 90% within the limits given by the 90% confidence interval, and that each new measurement can be found with a probability of 90% within the limits given by the 90% prediction interval. The 90% confidence interval for the activation energy of the intrinsic diffusion coefficient ranges from 4.096 to 4.311 eV.

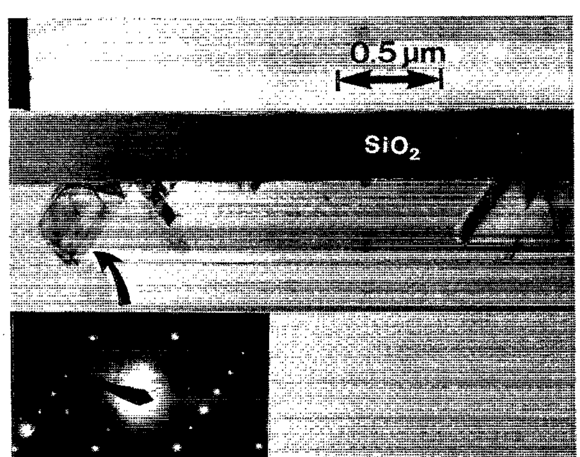

FIG. 6. Bright field XTEM image of the sample with doped polysilicon annealed at 950 °C for 28 h. The inset is the diffraction pattern showing the twinned structure of the defects.

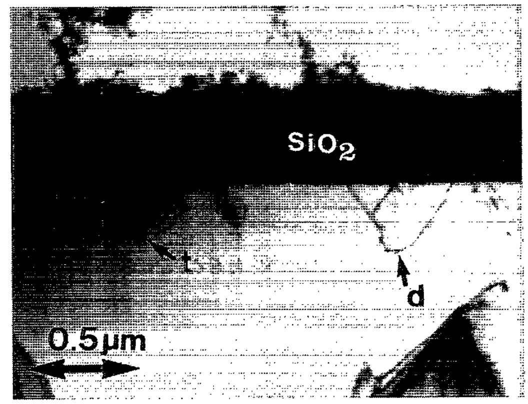

FIG. 7. Bright field XTEM image of the sample with doped polysilicon annealed at 1050 °C for 2 h. Twins (t) and dislocation loops (d) were found.

All diffusion coefficients determined from the wafers without an epitaxial layer are within the 90% prediction interval, and three of the four values are even within the 90% confidence interval. This is a clear indication that the effects seen in the other samples are physical effects rather than results of misprocessing.

The effective diffusion coefficients in the wafers with an epitaxial layer were found to be well below these intrinsic values. As mentioned in Sec. I, antimony diffuses nearly exclusively via vacancies. Thus it has to be concluded that the concentration of vacancies in the epitaxial layer during the final heat treatment was considerably lower than the equilibrium value.

It was further found that the diffusion of antimony was enhanced in wafers with a doped polysilicon layer (Fig. 1) in comparison to those without such a layer. This is in contradiction to previous experiments[10] where a retarded diffusivity of antimony was reported below regions with high phosphorus concentrations. Still, in samples doped with

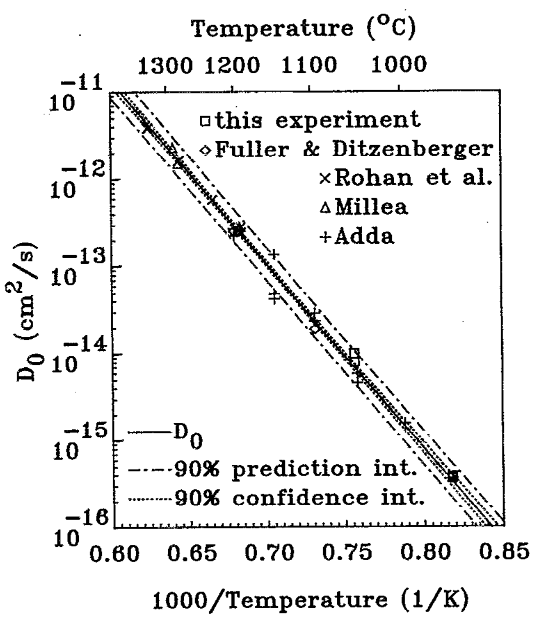

FIG. 8. Intrinsic diffusion coefficient of antimony.

TABLE II. Effective values δD_{eff} estimated from the effective diffusion coefficients in Table I.

		Without phosphorus	Phosphorus 3×10^{16} cm^{-2}	Phosphorus 2×10^{17} cm^{-2}
950 °C	FZ	−0.675	−0.467	0.154
	CZ	−0.645	−0.379	
1050 °C	FZ	−0.347	−0.173	
	CZ	−0.594	−0.478	

phosphorus to a dose of 3×10^{16} cm^{-2}, even these increased diffusivities are considerably lower than the respective intrinsic values.

Assuming local equilibrium between vacancies and self-interstitials, Tan and Gösele found that the relative diffusivity enhancement δD, i.e., the difference measured in units of the intrinsic diffusion coefficient of the dopants between their diffusion coefficient under nonequilibrium conditions and their intrinsic diffusion coefficient, can be expressed as a function of the relative oversaturation of self-interstitials, s_I, as

$$\delta D(s_I,f_I)\equiv\frac{D(s_I,f_I)-D_0}{D_0}=\frac{s_I}{s_I+1}\,(2f_I+f_Is_I-1). \quad (2)$$

f_I denotes the fraction of dopant diffusivity via self-interstitials with the limits of 1 for diffusion via self-interstitials alone and 0 for diffusion via vacancies alone. The relative oversaturation of self-interstitials, s_I, is defined via the concentration of self-interstitials, C_I, and the respective equilibrium concentration C_I^{eq} as

$$s_I=\frac{C_I-C_I^{\mathrm{eq}}}{C_I^{\mathrm{eq}}}. \quad (3)$$

From the effective diffusion coefficients reported in Table I and the values for the intrinsic diffusion coefficient determined above, effective values of δD_{eff} can be estimated and are listed in Table II.

Equation (2) has a minimum for $s_I>0$ when f_I takes values in the range $0<f_I<0.5$, as is the case for antimony. Figure 9 shows the relation for some values of f_I. The minimum of δD, δD_{min}, decreased monotonically with decreasing f_I. Because of the minimum in the $\delta D(s_I)$ curves, a measured mean value is always higher than δD_{min}. Thus the values in Table II can be used as upper limits for δD_{min} and, because of the monotonic relation between δD_{min} and f_I, upper values for f_I can be estimated straightforwardly from the values in Table II. The estimates $f_I\leq0.027$ at 950 °C and $f_I\leq0.043$ at 1050 °C include $f_I=0.02$ as proposed by Tan and Gösele[16] and $f_I=0.015$ as given by Antoniadis and Moskowitz,[17] both estimated for 1100 °C.

It can also be seen from Fig. 9 that the increased diffusivity of antimony in samples with implanted phosphorus can be interpreted in two ways, either by a reduced concentration of self-interstitials, i.e., an injection of vacancies, following the left branch of the curve, or by an additional injection of self-interstitials, following the right branch. To distinguish between the two possibilities, the different phos-

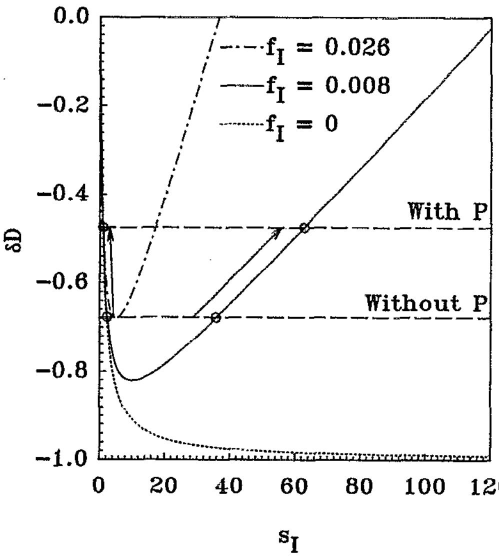

FIG. 9. Dependence of the relative diffusivity enhancement δD as a function of the relative oversaturation of self-interstitials s_I for specific values of the fractional diffusivity via self-interstitials f_I.

phorus and antimony profiles in the processed CZ and FZ samples can be used. These differences may be caused by variations in the epitaxy process, by bulk effects like oxygen precipitation, or by a different capturing capability of the polysilicon layers. Their true origin is of little concern for the following analysis as long as it can be assumed that these effects affect the point defect distributions similarly in the neighboring regions of the phosphorus tail and the antimony marker layer.

During heat treatment of the samples doped with phosphorus to a dose of 3×10^{16} cm^{-2} at 950 °C, the effective diffusion coefficient of antimony was smaller in the FZ sample than in the respective CZ sample. When we assume that phosphorus injects vacancies, following the left branch of the curve in Fig. 9, this means that the mean oversaturation of self-interstitials was higher in the FZ wafers. Since f_I has to be in the range from 0 to 0.027, it can be estimated that the observed relative diffusivity enhancement would correspond to effective values of s_I in the range from 0.88 to 1.0 for the FZ sample and from 0.61 to 0.69 for the CZ sample. Because of the problems mentioned with relating mean values for the relative diffusivity enhancement to mean values for the relative oversaturation of self-interstitials, these effective numbers are not directly mean values of the relative oversaturation of self-interstitials. Rather, they correspond to the value of s_I under the assumption that s_I is constant during the process. From Fig. 3, it can be seen that the effective diffusivity of phosphorus is lower in the FZ sample. A lower phosphorus diffusivity in connection with a higher oversaturation of self-interstitials would mean a value of $f_I<0.5$ for phosphorus. However, this would also mean that the relative diffusivity enhancement of phosphorus is negative for the possible values of the relative oversaturation of self-interstitials, i.e., the diffusion coefficient in the tail would be lower than D_0. Since this would not possibly lead to the observed kink and tail in the phosphorus profiles, the left branch of the $\delta D(s_I)$ curve can be ruled out conclusively at 950 °C.

At 1050 °C, in contrast to the experiments at 950 °C, assuming again an injection of vacancies from the high-concentration phosphorus region, the antimony data suggest a higher self-interstitial concentration in the CZ samples. At the same time, it can be seen from Fig. 4 that the effective diffusivity is higher in the FZ sample. Such a behavior is again possible only for $f_I<0.5$ where the relative diffusivity enhancement of phosphorus would be negative. Under such circumstances, the relative diffusivity enhancement of phosphorus would be negative which is a gain in contradiction to the shape of the profiles in Fig. 4.

Assuming an injection of self-interstitials from the phosphorus-doped region, following the right branch of the curve in Fig. 9, the decreased diffusivity of antimony at 950 °C in the FZ sample with respect to the respective CZ sample indicates a supersaturation of self-interstitials in the latter. Since the fractional diffusivity of phosphorus via self-interstitials is larger than for antimony, there will always be an increased diffusivity of phosphorus when the diffusivity of antimony is increased. This is in agreement with the observations of the diffusivities of phosphorus and antimony at both 950 and 1050 °C.

We thus conclude that the observed increased diffusivity of antimony below regions with phosphorus being present in large concentrations can be attributed only to an injection of self-interstitials. This conclusion replaces our erroneous conclusion published in the proceedings of ESSDERC'94[18] which was already corrected in the respective oral presentation.

From the phosphorus profile with a dose of 2×10^{17} cm^{-2} in Fig. 3 it can be seen that the phosphorus atoms were basically immobile within the first 150 nm of the polysilicon layer. The most likely reason is the formation of phosphorus precipitates. Below this region, the concentration corresponds to the solubility concentration of phosphorus in the crystalline silicon being in equilibrium with the phosphorus atoms in the precipitates. It can be estimated from Fig. 3 to be approximately 5×10^{20} cm^{-3}. In contrast, a phosphorus dose of 3×10^{16} cm^{-2} was not sufficient to maintain the solubility concentration in the crystalline region during the whole process.

A constant concentration at one boundary of the simulation area is a prerequisite[19] for a Boltzmann–Matano analysis.[20] Another prerequisite would be that the diffusion coefficient is a function of concentration only. This is virtually never the case in high-concentration phosphorus diffusion because of the interaction with the intrinsic point defects. Nevertheless, Boltzmann–Matano analysis is often used to estimate effective diffusivities in regions of a profile like in the tail regions of boron or phosphorus profiles.[21] The diffusivity at a certain concentration C_1 results from the profile diffused for at time t via

$$D(C_1)=-\frac{1}{2t}\frac{\int_0^{C_1}x\,dC}{(dC/dx)_{C=C_1}}. \quad (4)$$

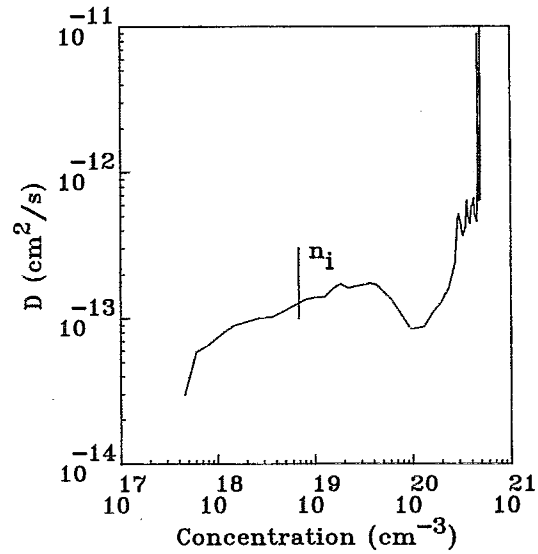

FIG. 10. Boltzmann–Matano analysis of the phosphorus profile after heat treatment at 950 °C for 28 h in the FZ sample with polysilicon doped with a phosphorus dose of 2×10^{17} cm^{-2}.

The result of the Boltzmann–Matano analysis for the phosphorus profile with the dose of 2×10^{17} cm^{-2} in Fig. 3 is shown in Fig. 10. Because of the uncertainty in the origin of the depth scale for such an analysis, analyses was performed assuming that the origin is at the interface between polysilicon and silicon or at the end of the implanted region where the peak at the surface drops to the solubility concentration. The results of both analyses were identical within the experimental error.

From Fig. 10, an effective tail diffusivity of 10^{-13} cm^2/s can be estimated for concentrations below the intrinsic value. Using the intrinsic diffusion coefficient of 3.39×10^{-15} cm^2/s from Fair,[22] the effective relative diffusivity enhancement of phosphorus in the tail can be estimated to be 28.5. Since the fractional diffusivity of antimony via self-interstitials has to be in the range from zero to 0.027, it can be estimated that the effective oversaturation takes values of $s_I\geqslant40.6$. From this value, together with the effective relative diffusivity enhancement of phosphorus in the tail region, it can be estimated that the fractional diffusivity of phosphorus via self-interstitials is smaller than 0.71.

The values of $f_I=0.02$ and $f_I=0.015$ for antimony reported by Tan and Gösele[16] and Antoniadis and Moskowitz[17] for 1100 °C would lead at 950 °C to estimates for phosphorus of $f_I\sim0.52$ and $f_I\sim0.39$, respectively. These values would fit to the value of $f_I=0.468$ at 950 °C given by Collard and Taniguchi[23] who, at 1100 °C, estimate a value of $f_I=0.846$. A value of $f_I=0.135$ as given by Mathiot and Pfister[24] would mean an effective oversaturation of $s_I\geqslant217$ for the diffusivity in the tail region. This would imply that the fractional diffusivity of antimony via self-interstitials has to be smaller than $f_I\leqslant0.0053$.

VI. CONCLUSIONS

In a series of experiments, it was found for the first time that diffusion of phosphorus in high concentrations from a polysilicon source increases the diffusivity of a spatially separated antimony marker layer. Differences between separately processed CZ and FZ wafers indicate that high-concentration phosphorus diffusion generates self-interstitials at both investigated temperatures of 950 and 1050 °C. This might be caused by phosphorus diffusing at high concentrations predominantly via self-interstitials, or because of the observed recrystallization of the polysilicon hampering its capability to capture intrinsic point defects possibly generated by phosphorus precipitation.

Using Boltzmann–Matano analysis and antimony diffusivity data, the fractional diffusivity of phosphorus via self-interstitials was estimated to be lower than 0.71 at 950 °C. Considering the experimental errors and the uncertainties involved in the Boltzmann–Matano analysis, the assumption of local equilibrium between self-interstitials and vacancies, and in the relation between effective oversaturation of self-interstitials and effective diffusion coefficients, it seems premature to draw a final conclusion concerning the fractional diffusivity of phosphorus via self-interstitials.

ACKNOWLEDGMENTS

Work at FhG-IIS-B and CEMES/LOE-CNRS was part of ADEQUAT (JESSI project BT1B) and was partly funded as ESPRIT Project No. 7236. One of the authors (P. P.) wants to thank Dr. N. Cowern, Professor U. Gösele, and Dr. D. Mathiot for the helpful discussions as well as all colleagues from the technology department of FhG-IIS-B who helped to make this experiment a success.

[1] L. E. Miller, *Properties of Elemental and Compound Semiconductors*, edited by H. C. Gatos, Metallurgical Society Conference Proceedings No. 5 (Interscience, New York, 1960), p. 303; T. H. Yeh, Bull. Am. Phys. Soc. **7**, 332 (1962); Y. Sato and H. Arata, Jpn. J. Appl. Phys. **3**, 511 (1964); R. Gereth, P. G. G. van Loon, and V. Williams, J. Electrochem. Soc. **112**, 323 (1965); J. E. Lawrence, J. Appl. Phys. **37**, 4106 (1966).
[2] E. Tannenbaum, Solid-State Electron. **2**, 123 (1961).
[3] M. C. Duffy, F. Barson, J. M. Fairfield, and G. H. Schwuttke, J. Electrochem. Soc. **115**, 84 (1968); J. C. C. Tsai, Proc. IEEE **57**, 1499 (1969); F. N. Schwettmann and D. L. Kendall, Appl. Phys. Lett. **21**, 2 (1972).
[4] M. Yoshida, Jpn. J. Appl. Phys. **10**, 702 (1971); J. Appl. Phys. **48**, 2169 (1977).
[5] R. B. Fair and J. C. C. Tsai, J. Electrochem. Soc. **124**, 1107 (1977).
[6] A. Seeger and K. P. Chik, Phys. Status Solidi **29**, 455 (1968).
[7] G. R. Booker and W. J. Tunstall, Philos. Mag. **13**, 71 (1966).
[8] P. Fahey, G. Barbuscia, M. Moslehi, and R. W. Dutton, Appl. Phys. Lett. **46**, 784 (1985).
[9] D. Mathiot and J. C. Pfister, Appl. Phys. Lett. **47**, 962 (1985).
[10] R. M. Harris and D. A. Antoniadis, Appl. Phys. Lett. **43**, 937 (1983); P. Fahey, R. W. Dutton, and S. M. Hu, *ibid.* **44**, 777 (1984); J. C. C. Tsai, D. B. Schimmel, R. B. Fair, and W. Maszara, J. Electrochem. Soc. **134**, 1508 (1987).
[11] R. Dürr and P. Pichler, Electrosoft **1**, 291 (1990).
[12] C. S. Fuller and J. A. Ditzenberger, J. Appl. Phys. **27**, 544 (1956).
[13] J. J. Rohan, N. E. Pickering, and J. Kennedy, J. Electrochem. Soc. **106**, 705 (1959).
[14] M. F. Millea, J. Phys. Chem. Solids **27**, 315 (1966).
[15] L. P. Adda, experimental data published by R. B. Fair, M. L. Manda, and J. J. Wortman, J. Mater. Res. **1**, 705 (1986).
[16] T. Y. Tan and U. Gösele, Appl. Phys. Lett. **40**, 616 (1982).
[17] D. A. Antoniadis and I. Moskowitz, J. Appl. Phys. **53**, 6788 (1982).
[18] P. Pichler, H. Ryssel, G. Wallmann, and R. Ploβ, *Proceedings of ESSDERC'94*, edited by C. Hill and A. Ashburn (Editions Frontieres, Gif-sur-Yvette Cedex, 1994), p. 89.
[19] H. S. Carslaw and J. C. Jaeger, *Conduction of Heat in Solids*, 2nd ed. (Clarendon, Oxford, 1984), pp. 89–90.
[20] L. Boltzmann, Ann. Phys. Chem. **53**, 959 (1894); C. Matano, Jpn. J. Phys. **8**, 109 (1933).
[21] E. Tannenbaum, Solid-State Electron. **2**, 123 (1961); G. L. Vick and K. M. Whittle, J. Electrochem. Soc. **116**, 1142 (1969); C. Kim, Z-Y. Zhu, R-I. Kang, and K. Shono, *ibid.* **131**, 2962 (1984); A. Sultan, M. Lobo, S. Bhattacharya, S. Banerjee, S. Batra, M. Manning, and C. Dennison, J. Electron. Mater. **22**, 1129 (1993).
[22] R. B. Fair, in *Impurity Doping Processes in Silicon*, edited by F. F. Y. Wang (North-Holland, Amsterdam, 1981), p. 315.
[23] D. Collard and K. Taniguchi, IEEE J. Electron Devices **ED-33**, 1454 (1986).
[24] D. Mathiot and J. C. Pfister, J. Appl. Phys. **55**, 3518 (1984).